J|A|C|S
ARTICLES
Published on Web 01/06/2006

Ultrafast Fluorescence Dynamics of Tryptophan in the Proteins Monellin and IIA^{Glc}

Jianhua Xu,[†] Dmitri Toptygin,[‡] Karen J. Graver,[†] Rebecca A. Albertini,[§] Regina S. Savtchenko,[‡] Norman D. Meadow,[‡] Saul Roseman,[‡] Patrik R. Callis,[§] Ludwig Brand,[‡] and Jay R. Knutson*,[†]

Contribution from the Optical Spectroscopy Section, Laboratory of Biophysical Chemistry, National Heart, Lung and Blood Institute, National Institutes of Health, Bethesda, Maryland 20892-1412, Department of Biology, Johns Hopkins University, 3400 North Charles Street, Baltimore, Maryland 21218, and Department of Chemistry and Biochemistry, Montana State University, Bozeman, Montana 59717

Received August 22, 2005; E-mail: jaysan@helix.nih.gov

Abstract: The complete time-resolved fluorescence of tryptophan in the proteins monellin and IIA^{Glc} has been investigated, using both an upconversion spectrophotofluorometer with 150 fs time resolution and a time-correlated single photon counting apparatus on the 100 ps to 20 ns time scale. In monellin, the fluorescence decay displays multiexponential character with decay times of 1.2 and 16 ps, and 0.6, 2.2, and 4.2 ns. In contrast, IIA^{Glc} exhibited no component between 1.2 ps and 0.1 ns. For monellin, surprisingly, the 16 ps fluorescence component was found to have positive amplitude even at longer wavelengths (e.g., 400 nm). In conjunction with quantum mechanical simulation of tryptophan in monellin, the experimental decay associated spectra (DAS) and time-resolved emission spectra (TRES) indicate that this fluorescence decay time should be ascribed to a highly quenched conformer. Recent models (Peon, J.; et al. *Proc. Natl. Acad. Sci. U.S.A.* **2002**, *99*, 10964) invoked exchange-coupled relaxation of protein water to explain the fluorescence decay of monellin.

Introduction

Fluorescence spectroscopy is widely used to study both the structure and dynamics of biomolecules which may be linked to function.[1,2] To examine peptide and protein environments and conformation changes, tryptophan (Trp), the most important fluorophore among amino acids, has been the subject of photophysical studies for decades.[3,4] The fluorescent moiety (indole) possesses the highest UV extinction coefficient among amino acids and generally has the highest fluorescence quantum yield.[5] The lowest singlet state (the ^1L_a state) is sensitive to the polarity and dynamics of the immediate environment.[6] The emission wavelength maximum of Trp in proteins varies from 308 to 355 nm, as the extent of exposure to water increases (more generally, it reflects the local electrostatic environment).[7] Many peptides and proteins containing single Trp residues have wavelength-dependent multiexponential fluorescence decays, with each exponential term providing a different decay associated spectrum (DAS).[3,8,36] To interpret decay surfaces, one starts with the realization that two distinct sources can yield exponential terms: (1) excited population loss, i.e., "population decay"; (2) equilibration of the suddenly prepared excited state leading to spectral shifts without change in overall excited state population. These we refer to broadly as solvent relaxation (protein may contribute, too). The competing models for multiexponential fluorescence decay depend on which kinetic process dominates and on the role of heterogeneity. Multiple population decay rates are most simply explained on the basis of ground-state heterogeneity due to the presence of several conformers, each with distinct environments and different fluorescence lifetimes.[9−11]

Comparison of preexponential terms with NMR-derived angular population data has supported a "rotamer" view.[11,12] In this view, side-chain rotamers that do not exchange on the fluorescence time scale constitute the source of ground-state heterogeneity.

An alternative model is based solely on solvent relaxation on the nanosecond scale arising from the increased dipole

[†] National Institutes of Health.
[‡] Johns Hopkins University.
[§] Montana State University.

(1) Frauenfelder, H.; Sligar, S. G.; Wolynes, P. G. *Science* **1991**, *254*, 1598.
(2) Carerri, G.; Fasella, P.; Gratton, E. *Annu. Rev. Biophys. Bioeng.* **1979**, *8*, 69.
(3) Beechem, J. M.; Brand, L. *Annu. Rev. Biochem.* **1985**, *54*, 43.
(4) Lakowicz, J. R. *Principles of Fluorescence Spectroscopy*, 2nd ed.; Kluwer Academic/Plenum Publishers: New York, 1999.
(5) Cantor, C. R.; Schimmel, P. R. *Biophysical Chemistry Part II*; W. H. Freeman: New York, 1980.
(6) Callis, P. R. *Methods Enzymol.* **1997**, *278*, 113.
(7) Longworth, J. W. In *Time-Resolved Fluorescence Spectroscopy in Biochemistry and Biology*; Cundall, R. B., Dale, R. E., Eds.; Plenum: New York, 1983; p 672.
(8) Rayner, D. M.; Szabo, A. G. *Can J. Chem.* **1978**, *56*, 743.
(9) Szabo, A. G.; Rayner, D. M. *J. Am. Chem. Soc.* **1980**, *102*, 554.
(10) Ross, J. A.; Wyssbrod, H. R.; Porter, R. A.; Schwartz, G. P.; Michaels, C. A.; Laws, W. R. *Biochemistry* **1992**, *31*, 1585.
(11) Mcmahon, L. P.; Yu, H. T.; Vela, M. A.; Morales, G. A.; Shui, L.; Fronczek, F. R.; McLaughlin, M. L.; Barkley, M. D. *J. Phys. Chem. B* **1997**, *101*, 3269.
(12) Clayton, A.; Sawyer, W. *Biophys J.* **1999**, *76*, 3235.

10.1021/ja055746h CCC: $33.50

moment of the excited state.[13−15] This model necessarily yields relatively short-lived "blue" and long-lived "red" DAS [DAS, Decay Associated Spectr(a)um: spectra composed of amplitudes for each decay function]. It also yields an average lifetime that increases with increasing observation wavelength[16] and sets of decay associated spectra that are ordered with longer decay times linked to longer wavelength components. The latter trend (ordering of DAS with decay times) has, in fact, been observed in most single Trp proteins. The heterogeneous population decay viewpoint of proteins, however, has been buttressed by recent lifetime studies on constrained Trp derivatives[17] and on protein crystals[18] that display a rational (trigonometric) dependence of preexponential amplitudes upon rotation. Also supporting this view is the reduced number of exponentials seen when Trps with short lifetimes in one protein were replaced by 5FTrp[19] (a modification that arguably reduces ET rates), while no reduction in complexity was seen for a Trp with a long lifetime in another protein.[20] The simplification sought with 5FTrp, of course, applies to electron transfer heterogeneity, so either complex solvation or the persistence of other (non-ET) quenching mechanisms might keep these curves multiexponential. Trp replacements with nonnative chromophores bearing larger dipole moments have also been employed to explore solvation.[21]

Fortunately, solvation in proteins often precedes the emergence of population heterogeneity. Separating the two kinetic processes (population vs relaxation) can be difficult if they overlap in the experimental time window. Every unknown Trp environment should be approached with both models in mind.

The popularity of shorthand terms "rotamer model" and "solvent relaxation" should not restrict either model unnecessarily. In addition to explicit rotamers of the Trp side chain, one must recognize that *microconformational* states of proteins with different local environments of the indole ring constitute a source of ground-state heterogeneity (i.e., in proteins, we should discuss "conformers" instead of "rotamers"). Regarding solvent relaxation, motions of *either* the protein matrix or solvent water near the indole ring can produce complex decay, and they are strongly coupled.

In the general spectral relaxation case, as one scans across the emission spectrum, decay curves should continuously change from those with more rapid decay at the (depleting) blue end of the spectrum, to a region where the average population lifetime is dominant, and finally to rising behavior at the red end of the spectrum (i.e., the blue side is losing population both to spontaneous decay and relaxation, the center is less complex, and the red side accumulates relaxed molecules quickly prior to decay). On the red edge, this kinetic behavior yields a negative preexponential amplitude associated with a short lifetime ("short negative DAS region"), and it is diagnostic of an excited-state reaction.[42] Of course, the lack of a negative amplitude does not *rule out* relaxation, as plausible models can be constructed where spectral overlap will work to suppress that signature.

Computer simulations can also guide the modeling process. Molecular dynamics runs previously made for solvent relaxation of 3-methylindole in water revealed bimodal character; there was an ultrafast Gaussian response of ∼15 fs (from trajectory changes "between collisions" of adjacent solvent molecules), followed by a relatively slower exponential response of ∼400 fs due to diffusive motion.[22−24] Recent instrument developments have permitted clarification of such picosecond events, such as ∼1.2 ps bulk water relaxation around Trp.[24,25]

Monellin is one of the proteins with high affinity for the human sweet taste receptor, so it has been studied to understand the mechanism of taste. Monellin has two polypeptide chains associated by H−bonding and hydrophobic regions. Chain A is 45 residues, and chain B has 50 residues, including Trp at position 3. It is noted that there are seven tyrosines near the Trp in monellin, two of which are within 9 Å.

IIA^{Glc} (formerly known as III^{Glc})[26−30] is a phospho-carrier protein of the bacterial phosphoenolpyruvate: glycose phosphotransferase system (PTS) from *Escherichia coli*. It has a well-defined solution structure, which consists of a rigid globule of residues 19 through 168 and a flexible tail comprising the first 18 residues. The native IIA^{Glc} has neither Trp nor tyrosine residues. For the mutant E21W, a Trp residue was inserted at the end of the rigid globule, therefore, E21W has just one Trp and no tyrosine, which helps to avoid permanent heterogeneity and precludes complications due to conceivable tyrosine-to-tryptophan energy transfer. The latter is important whenever one excites a protein such as monellin below 295 nm; Tyr is easily quenched by Förster resonance energy transfer to Trp, and this can yield negative preexponentials in Trp decay curves that are due only to FRET. These terms can either appear as negative (rising) decay or counter other positive terms (with similar decay times).

In this paper, a wide range of spectral and lifetime data for the single Trp residues in monellin and IIA^{Glc} has been gathered to more fully understand their photophysics. In addition to conventional absorption spectra and steady-state fluorescence measurements, time-resolved fluorescence transients, including fluorescence decay curves and decay associated spectra, are obtained using both an upconversion spectrophotofluorometer and a time-correlated single photon counting (TCSPC) apparatus coupled to femtosecond and picosecond laser sources. The dynamics are dissected to reveal contributions from both the heterogeneous Trp environs of the protein and the evolving solvent shell. In addition to a "*bulk water*" relaxation of 1.2 ps found in both proteins, a 16 ps fluorescence component exclusive to monellin was found with positive decay amplitude evident even at longer wavelengths (e.g., 400 nm). As described

(13) Alcala, J. R.; Gratton, E.; Prendergast, F. G. *Biophys. J.* **1987**, *51*, 925.
(14) Vincent, M.; Gallay, J.; Demchenko, A. P. *J. Phys. Chem.* **1995**, *99*, 14931.
(15) Toptygin, D.; Savtchenko, R.; Meadow, D.; Brand, L. *J. Phys. Chem. B* **2001**, *105*, 2043.
(16) Lakowicz, J. R. *Photochem. Photobiol.* **2000**, *72*, 421.
(17) Adams, P. D.; Chen, Y.; Ma, K.; Zagorski, M. G.; Sonnichsen, F. D.; McLaughlin, M. L.; Barkly, M. D. *J. Am. Chem. Soc.* **2002**, *124*, 9278.
(18) Dahms, T. E. S.; Willis, K. J.; Szabo, A. G. *J. Am. Chem. Soc.* **1995**, *117*, 2321.
(19) Liu, T.; Callis, P. R.; Hesp, B. H.; de Groot, M.; Buma, W. J.; Broos, J. *J. Am. Chem. Soc.* **2005**, *127*, 4104.
(20) Toptygin, D.; Gronenborn, A. M.; Brand, L. *Biophys. J.* **2005**, *88A*, 161.
(21) Cohen, B. E.; McAnaney, T. B.; Park, E. U.; Jan, Y. N.; Boxer, S. G.; Jan, L. Y. *Science* **2002**, *296*, 1700.
(22) Muino, P. L.; Callis, P. R. *J Chem. Phys.* **1994**, *100*, 4093.
(23) Jimenez, R.; Fleming, G. R.; Kumar, P. V.; Maroncelli, M. *Nature* **1994**, *369*, 471.
(24) Shen, X.; Knutson, J. R. *J. Phys. Chem. B* **2001**, *105*, 6260.
(25) Lu, W.; Kim, J.; Qiu, W.; Zhong, D. *Chem. Phys. Lett.* **2004**, *388*, 120.
(26) Pelton, J. G.; Torchia, D. A.; Remington, S. J.; Murphy, K. P.; Meadow, N. D.; Roseman, S. J. *Biol. Chem.* **1996**, *52*, 33446.
(27) Pelton, J. G.; Torchia, D. A.; Meadow, N. D.; Wong, C. Y.; Roseman, S. *Biochemistry* **1991**, *30*, 10043.
(28) Pelton, J. G.; Torchia, D. A.; Meadow, N. D.; Wong, C. Y.; Roseman, S. *Proc. Natl. Acad. Sci. U.S.A.* **1991**, *88*, 3479.
(29) Meadow, N. D.; Roseman, S. J. *Biol. Chem.* **1982**, *257*, 14526.
(30) Worthylake, D.; Meadow, N. D.; Roseman, S.; Liao, D. I.; Herzberg, O.; Remington, S. J. *Proc. Natl. Acad. Sci. U.S.A.* **1991**, *88*, 10382.

below, the confluence of data and simulations will favor assignment of this term to a quenched conformer. It was previously argued that the time constant of 16 ps mirrored relaxation of an exchanging surface-bound water layer.[31] Recently, Larsen et al. have also found a ~16 ps fluorescence component for Trp in a small 22-mer peptide, and they proposed that this lifetime originated from a rotamer of Trp, [32] which is in agreement with our findings. We have studied several dipeptides and found that quasi-static self-quenching (QSSQ)[33] often leads to sub-100 ps decay terms[34] that can now be used to rationalize yield "defects". Those yield defects (vs lifetime) were once thought to track variations in radiative rate.

Experimental Section

Upconversion Spectrophotofluorometer. In this system, a mode-locked Ti:sapphire laser (Tsunami, Spectra-Physics) pumped by an argon ion laser (Beamlock 2060, Spectra-Physics) was used to generate a 300−600 mW pulse train with a typical pulse duration of 120 fs at a repetition rate of 82 MHz. The oscillator wavelength was tunable from 800 to 900 nm. The pulses were used to seed a Ti:sapphire regenerative amplifier (Spitfire, Spectra Physics). The amplified pulses at 885 nm had an energy of ~140 μJ and an autocorrelation pulse width of 350 fs at a repetition rate of 5 kHz. Our "far red optics" modified amplifier was tunable between 865 and 905 nm. The blue side is restricted by cavity mirrors chosen to quench self-Q switching, the red side by gain pulling. Ultraviolet excitation with an average power up to 30 mW was obtained from nonlinear frequency conversion using a 1 mm BBO crystal and 0.5 mm BBO crystal for doubling and tripling, respectively. The UV beam (tripled) was separated from the infrared beam (fundamental), and blue beam (doubled) by two dichroic mirrors, and the power was carefully attenuated before excitation of the sample to avoid photodegradation, hole burning, and other undesirable effects (see below). The sample was held in a circular array of thin cells (T-20, NSG Precision Cells) with a path length of 1 mm in a continuously (>5 m/s) spinning delrin stacked slotted disk. The residual fundamental pulse was retroreflected from a hollow cube corner on a computer-controlled precision stage, and this variably delayed pulse was used as a gate pulse for the upconversion process. The fluorescence emission was collected and focused into a 0.2 mm thick BBO mixing crystal, and the upconversion signal was produced via type I sum frequency generation with the gate pulse in the crystal. To reject the strong background signals (infrared laser, remnant UV, and unconverted fluorescence) accompanying the upconverted signal, a noncollinear configuration was arranged between infrared laser and fluorescence. Polarizations of gated fluorescence were determined by the orientation of nonlinear crystals; no extra linear polarizer was needed. The polarization of the excitation beam was chosen by a motor-controlled zero-order half-wave plate. Hence there were no elements in the collection train apt to induce polarization bias (for anisotropy calculation, $G \sim 1$.). By angle tuning the mixing crystal, the upconverted fluorescence, with a wavelength in the range of 230−280 nm, always polarized in the same direction, was directed into a monochromator (Triax 320, Jobin Yvon Inc. with a bandwidth of 0.5 nm) and a solar blind photomultiplier tube (R2078, Hamamatsu, dark rate < 1 cps). Amplified SBPMT signals were discriminated and then recorded by a gated single photon counter (994, EG&G Ortec). Photon arrival events were held to less than 5% of the repetition rate to minimize "pileup". The "lamp" (AKA "apparatus" or "instrument response") function was determined by measuring the cross-correlation either between the UV and infrared pulses or (routinely, and more precisely) between UV-generated spontaneous Raman scattering in water and the infrared pulse. In both ways, the lamp function was found to be around 450 fs (fwhm), with a timing jitter of less than 30 fs. When collecting on longer time scales, detuning to ~1 ps fwhm was occasionally done to optimize other parameters. Instrument calibration was verified with the linear fluorophore, *p*-terphenyl, which yielded an initial anisotropy of 0.40 ± 0.01 and a single rotational correlation time of 41 ps in cyclohexane (both from Sigma/Aldrich).

TCSPC Apparatus. A tunable Spectra-Physics Model 3500 cavity dumped dye laser was synchronously pumped by a frequency-doubled, mode-locked NdYVO4 laser (Vanguard 2000-HM532, Spectra-Physics). The dye laser output was doubled into the ultraviolet via an Inrad autotracker with BBO crystal. For the present work, rhodamine 6G was the laser dye used at 590 nm, and magic angle emission/vertical excitation was employed at 295 nm with pulses having a fwhm < 2 ps. The fluorescence was recorded from 310 to 405 nm via JYH10 monochromator with 8 nm bandwidth and a cooled MCP photomultiplier. The aggregate instrumental response time width was about 100 ps, so measurement of lifetimes of 50 ps and greater is possible in this instrument. Melatonin in water was used as a monoexponential standard. Lifetimes were obtained by fitting the decay data to a multiexponential model, according to the weighted nonlinear least-squares method.[21] Goodness of fit was assessed with the inspection of residuals and their autocorrelation and χ_R^2 functions.[35] (The fits employed in this work yielded values of 1.01−1.3.) For decay associated spectra (DAS),[35] a time-resolved decay surface was obtained on monellin by excitation at 295 nm and observation every 5 nm over the emission band. The instrument response function was contemporaneously obtained with a light-scattering suspension of dilute colloidal silica. Alternating the sample with the scatterer, stepping of the emission monochromator, data collection, and transfer of data from the multichannel buffer/analyzer to the computer was done automatically (program "DAS32"). In the analysis of the multiple curves obtained for a DAS, all were satisfactorily fit to the same global triple-exponential model.[37]

Steady-state absorption and fluorescence spectra were recorded with a diode array spectrophotometer (HP 8452A) and Fluorolog-3 spectrophotofluorometer (SPEX), respectively. The DAS and TRES were calibrated by normalizing our steady-state spectrum of Trp in water to spectra taken on another fluorometer previously referenced to a standard blackbody.

Samples. E21W, the mutant of protein IIA^{Glc}, was prepared as before.[15] The concentration of E21W in buffer, which contained no glycerol, was about 0.08 mM. Trp and the protein monellin were purchased from Sigma-Aldrich Chemical Co. They were used without further purification. The solutions were prepared in a 10 mM Na_2HPO_4/NaH_2PO_4 buffer at pH 7.2 using distilled deionized water. A typical concentration of Trp in water for upconversion was 1 mM. The monellin solutions were passed through a 0.45 μm sterile filter (Swinnex-HA) to remove insoluble particles from the solution. The concentration of monellin was determined to be 0.2 mM using the extinction coefficient $\epsilon_{277} = 1.46 \times 10^4\ M^{-1}\ cm^{-1}$.[38] All samples were made at room temperature. A fresh sample solution was prepared for each time-resolved measurement.

Simulation Methods

Solvent Relaxation. We have performed QM−MM simulations of monellin starting with the X-ray structure (pdb code 1MOL, a single chain mutant) solvated in a 31 Å radius sphere of explicit TIP3 water. Methods and procedures follow closely those of Callis et al.,[39] except that a quantum mechanical

(31) Peon, J.; Pal, S. K.; Zewail, A. H. *Proc. Natl. Acad. Sci. U.S.A.* **2002**, *99*, 10964.
(32) Larsen, O. F. A.; van Stokkum, I. H. M.; Pandit, A.; van Grondelle, R.; van Amerongen, H. *J. Phys. Chem. B* **2003**, *107*, 3080.
(33) Chen, R. F.; Knutson, J. R.; Ziffer, H.; Porter, D. *Biochemistry* **1991**, *30*, 5184.
(34) Xu, J.; Knutson, J. R. *Biophys. J.* **2003**, *84* (2), 287A.
(35) Badea, M. G.; Brand, L. *Methods Enzymol.* **1979**, *61*, 378.
(36) Knutson, J. R.; Walbridge, D. G.; Brand, L. *Biochemistry* **1982**, *21*, 4671.
(37) Knutson, J. R.; Beechem, J. M.; Brand, L. *Chem. Phys. Lett.* **1983**, *102*, 501.
(38) Morris, J. A.; Cagan, R. H. *Proc. Soc. Exp. Biol. Med.* **1980**, *164*, 351.

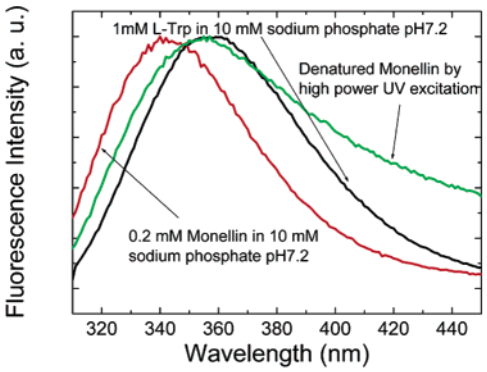

Figure 1. Normalized fluorescence spectra of Trp in water, in monellin, and purposely photodamaged monellin.

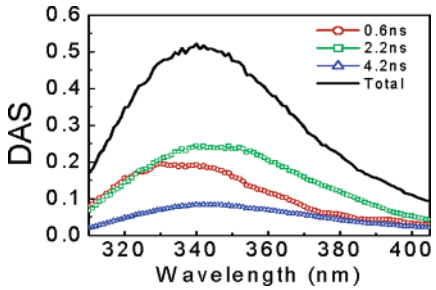

Figure 2. Decay associated spectra of Trp in monellin extracted from TCSPC data (0.6, 2.2, and 4.2 ns). Solid line, sum of these preexponential amplitudes (equivalent to spectrum seen by TCSPC instrument at "time zero").

calculation was made after each 1 fs step; 26 10-ps trajectories were averaged, each starting after a different equilibration time that varied from 1 to 5 ps. Each trajectory began with the Trp in the ground electronic state. After 50 fs, the system was put in the ^1L_a excited state.

For analysis during the first 1 ps of relaxation, a separate set of trajectories was run for which the starting conditions were identical and the system was left in the ground state.

Population Decay. Electron transfer rates were estimated following the method recently used to semiquantitatively predict fluorescence lifetimes and quantum yields for Trp in several proteins.[44−46] For monellin, the 1MOL structure was again used and for IIA^{Glc} 1F3G was used. Glu21 was mutated to Trp using Swiss PDB Viewer.

Results and Discussion

Steady State. Figure 1 shows the steady-state emission spectrum (295 nm excitation) of Trp in monellin and water, respectively. Monellin has a typical indole absorption band at 280 nm, although it lacks a shoulder near 290 nm, likely due to the seven tyrosines also present (data not shown). The fluorescence of monellin solution has its maximum at 342 nm, which is blue shifted relative to that of Trp in water (355 nm), in agreement with previous experiments.[31,42] Figure 1 also shows the fluorescence spectrum of Trp in monellin after it was intentionally exposed to a high average power UV beam (0.2 W/cm^2 for 2 h) in the upconversion system. It shows a significant peak shift to 352 nm with a big "tail" (likely a photoproduct) apparent at the red side. This change is associated with denaturation of the protein and photodegradation. To avoid this distortion, the UV beam in subsequent upconversion experiments was reduced to <1 mW (0.08 W/cm^2), exposures were minimized and pre-/post-run spectra (both absorbance and emission) were monitored. Moreover, a fresh sample was used for each wavelength during the upconversion DAS collection.

Nanosecond DAS/TRES of IIA^{Glc}. The E21W mutant of IIA^{Glc}, a tyrosine-free protein component of the bacterial PTS system, has been previously studied as a model for Trp relaxation on the nanosecond time scale.[15] In particular, decay surfaces with ~65 ps resolution were collected to high precision, permitting the detection of multiple DAS with small negative amplitudes on the red side of the emission spectrum. Equally important, a succession of TRES with *unchanged energy width* emerged from the proper translation of these DAS. Large negative amplitudes are a definitive signature of excited state redistribution of energy (e.g., relaxation); TRES of nearly constant width (in energy) are a necessary, but not sufficient, condition for a continuous relaxation model. Thus, on the 50 ps to 20 ns time scale, E21W exhibited DAS and TRES compatible with slow dipolar relaxation.[15]

Nanosecond DAS/TRES of Monellin. On the time scale from 100 ps to 20 ns, the decay curves of Trp in monellin are multiexponential. The decay profile was globally fitted using three lifetimes (0.6, 2.2, and 4.2 ns) with different DAS (decay associated spectra; see Figure 2). The central intensity-weighted mean lifetime $\langle\tau\rangle$[33] is around 2 ns, in agreement with previous investigation.[41] For comparison, Trp in water yielded a biexponential with lifetimes of 0.6 and 3.2 ns (data not shown), with a mean lifetime of ~3 ns.[9]

DAS are often useful for diagnosing the relative importance of heterogeneity versus relaxation in Trp emission. A positive/negative DAS is a classic hallmark of a two-state excited state reaction.[33] Figure 2 shows the decay associated spectra for Trp in monellin. The lifetimes (0.6, 2.2, and 4.2 ns) were obtained by fitting all the curves, rather than a single curve, to a global three exponential model. Since the DAS are all positive and do not shift in ascending lifetime order, we know heterogeneity is important here. As will be shown below, TRES width changes in this (0.1−20) nanosecond time range, an even stronger indicator the three lifetimes come from *heterogeneity*. The simplest explanation compatible with this finding is different conformers providing distinct environments for Trp.[33]

Femtosecond Upconversion Data for IIA^{Glc}. We expected that upconversion would reveal distinctive relaxation signatures on the 400 fs to 100 ps time scale. As shown in Figure 3A and B, single transients of the E21W protein yielded the characteristic blue positive/red negative 1.2 ps exponential previously seen for Trp solvation in bulk water.[30] Neither side of the spectrum exhibited terms slower than 2 ps that could be attributed to the exchange of bound water,[26] except for previously studied decay terms well over 50 ps (e.g., in the TCSPC range previously studied). We questioned whether the partially exposed nature of E21W could have rendered it less sensitive to such signals. Although the femtosecond response of this

(39) Vivian J. T.; Callis, P. *Biophys. J.* **2001**, *80*, 2093.
(40) Brand, J. G.; Cagan, R. H.; Bayley, D. L. *Proc. Soc. Exp. Biol. Med.* **1985**, *179*, 76.
(41) Swaminathan, R.; Krishnamoorthy, G.; Periasamy, N. *Biophys. J.* **1994**, *67*, 2013.
(42) Davenport, L.; Knutson, J. R.; Brand, L. *Biochemistry* **1986**, *25*, 1186.
(43) Shen, X.; Knutson, J. R. *Chem. Phys. Lett.* **2001**, *339*, 191.
(44) Kurz, L. C.; Fite, B.; Jean, J.; Park, J.; Erpelding, T.; Callis, P. *Biochemistry* **2005**, *44*, 1394.
(45) Callis, P. R.; Vivian, J. T. *Chem. Phys. Lett.* **2003**, *369*, 409.
(46) Callis, P. R.; Liu, T. *J. Phys. Chem. B* **2004**, *108*, 4248.

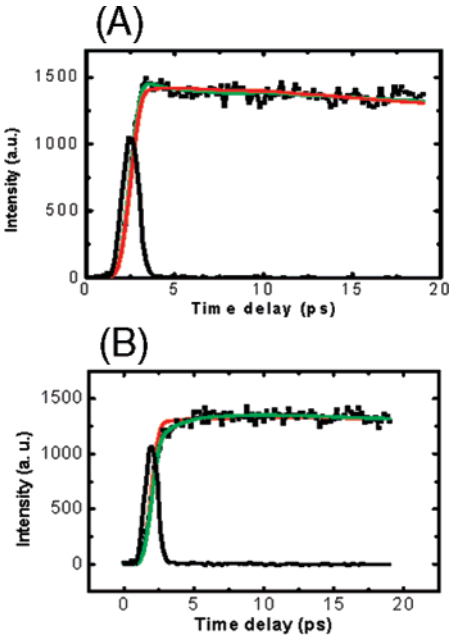

Figure 3. Representative fluorescence intensity decays for E21W protein at different wavelengths, 345 nm (A) and 375 nm (B), after excitation at 295 nm. The fluorescence decay can be fit (green lines) by $I(t) = 0.12 \exp(-t/1.3) + \exp(-t/240)$ at 345 nm, and $I(t) = -0.26 \exp(-t/1.5) + \exp(-t/210)$ at 375 nm, respectively (all terms in picoseconds). The red line is a monoexponential decay fit.

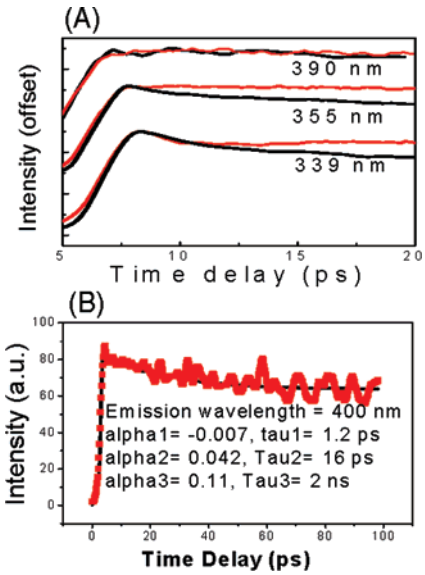

Figure 4. (A) Representative upconverted fluorescence intensity decay for Trp in water (red lines) and in monellin (black lines) at wavelengths of 339, 355, 390 nm using excitation at 295 nm. The fluorescence decay of Trp in monellin can be adequately fit by $I(t) = \alpha_1 \exp(-t/1.2) + \alpha_2 \exp(-t/16) + \alpha_3 \exp(-t/2000)$, and that of Trp in water can be fit by $I(t) = \alpha_1 \exp(-t/1.2) + \alpha_2 \exp(-t/3000)$, respectively (all terms in picoseconds). (B) Representative fluorescence intensity decay analysis for Trp in monellin (red data points) at the wavelength of 400 nm. The black line is three exponential decay fit: $I(t) = -0.007 \exp(-t/1.2) + 0.042 \exp(-t/16) + 0.11 \exp(-t/2000)$.

protein mimics Trp in water, steady-state iodide quenching of IIAGlc-E21W yielded a Stern−Volmer constant only approximately twice that of monellin (data not shown).

Femtosecond Upconversion DAS/TRES of Monellin. Figure 4A shows subpicosecond resolution fluorescence decays (20 ps full range) at three representative wavelengths for monellin solution (black lines) and Trp solution (red lines). The data in this figure were offset, and the peak was normalized for easy comparison. Clearly, monellin displays a decay process not seen with Trp alone. At 390 nm, it is difficult to see this process clearly. In Figure 4B, the temporal window we used for fitting the profile was increased to 100 ps. The 16 ps term is more visible in Figure 4B, and the fit including a positive 16 ps exponential is also shown. In this time window, we found good agreement between data at all fluorescence wavelengths and a two exponential decay fit for Trp in water versus three exponentials for monellin. One of these decay components was, of course, very slow on this interval (e.g., a step function). One may fix this time constant to the mean lifetimes of 3 ns (in water) or 2 ns (in monellin), without changing fit quality (the time window of observation is far shorter than these nanosecond decay constants).

As mentioned above, a "positive blue/negative red" DAS profile is diagnostic for relaxation. All the femtosecond transients clearly exhibited a fast decay at "bluer" emission wavelengths and a fast rise at "redder" emission wavelengths—*but only in the initial 5 ps*. Trp in water displayed only this fast water relaxation (∼1.2 ps) and a very slow (nanosecond) component in our work.[24] Clearly, the data for Trp in monellin cannot be fit satisfactorily without the use of an additional *ultrafast* component. More important, this decay component (16 ps) shows a *positive amplitude* (declining) exponential curve even at the red side of the spectrum (Figure 4B).

Femtosecond DAS. We extracted femtosecond DAS of Trp in monellin by normalizing upconversion data to the TCSPC "time zero" DAS.[42] Since the nanosecond decay of monellin was reconciled with unique decay times of ∼0.6, 2.2, and 4.2 ns, we can simply sum total preexponential amplitude of tryptophan in monellin (which differs from the steady-state spectrum) to obtain a spectrum at "zero" nanosecond time.[9] Of course, this time zero comes after the ∼1.2 ps solvent relaxation and 16 ps fast decays seen via upconversion; both are too fast to be observed by TCSPC instruments. We properly normalize the tails of our upconversion data curves to this zero time spectra, not the steady-state spectrum (as matching tails to I_{ss} incorrectly presumes a lack of nanosecond decay complexity). To normalize, one simply ratios the amplitude for the upconversion long lifetime of Trp in monellin (2 ns) with the amplitude of total TCSPC DAS (black line in Figure 2) representing "zero nanosecond time". To reiterate, at this time, intermediate between upconversion and TCSPC, solvent relaxation, and 16 ps decay are complete, while nanosecond shifts are not yet in play. The properly normalized femtosecond DAS thus extracted from upconversion data are shown in Figure 5. Note that the "bulk" water relaxation term (∼1.2 ps component) has both a positive and negative region in its DAS (blue squares) at the low wavelength and high wavelength sides, respectively. Interestingly, the novel (∼16 ps) component (green diamonds) has a *significant positive amplitude* in the longer wavelength region, and the spectrum is not significantly distorted (in fact, it resembles the 0.6 ns DAS of Figure 2). Solvent relaxation on the 16 ps time scale should have resulted in a positive/negative DAS, or at least a severely blue shifted DAS without a significant positive amplitude at 400 nm. As an aside, one need not include model terms for internal conversion between ^1L_b and ^1L_a since that process has been found to be much faster than 50 fs.[43]

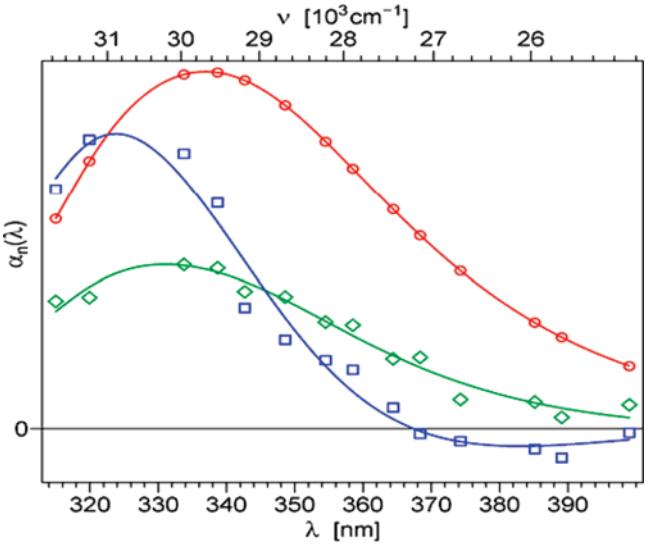

Figure 5. Raw decay associated spectra of Trp in monellin extracted from upconversion data (symbols) superposed with their polynomial fits (lines) (1.2 ps, blue; 16 ps, green; and 2 ns, red.)

Integrating data from both instruments, Figure 6 shows the properly normalized TRES (time-resolved emission spectra) across the full scale from 0.3 ps to 10 ns. Clearly, these TRES are not shifting homogeneously, as their energy width (red line in Figure 6C) varies dramatically after about 5 ps. Comparison with a known solvent relaxation process (indole/glycerol) is provided by blue lines in Figure 6C and D. The blue lines are based on previously published data.[48] Note that solvent relaxation results in a smooth uniform spectral shift on the logarithmic time scale. The monellin surface, in contrast, cannot be represented by uniform TRES shifting smoothly in time.

While our normalization methods differ, precluding direct comparison, we note that previously published monellin TRES[31] have qualitatively similar features to those shown here.

Simulation Results

Fluorescence Shift Dynamics. Figure 7 displays the average of 26 simulations after entry into the ^1L_a state. In these simulations, the system is taken instantaneously from the ground state directly to the ^1L_a state because internal conversion from a mixed ^1L_b−^1L_a excitation state of Trp in water to ^1L_a has been reported to occur in under 80 fs[24] (probably under 30 fs). The spectral shift in Figure 7 is adequately fit by the sum of a Gaussian (40% of shift) with 15 fs standard deviation along with an exponential term of ∼0.5 ps. One cannot exclude small (∼10%) subsequent energy shifts, but significant relaxation slower than ∼2 ps is not seen. Because the ultrafast Gaussian term is not observable with upconversion instruments (it could not be measured except with ∼20 fs pulses whose Heisenberg-implied spectral width would blanket the UV bands of Phe, Tyr, and Trp), we have included in Figure 7 only fits starting at 400 fs. Even looking at the 25% remaining (below 0.25) relaxation, one can state that the correlation function shown in Figure 7 certainly contains <20% relaxation slower than 2 ps. For comparison, Figure 7 also includes the shape of $C(t)$ (50% τ = 2 ps, 50% τ = 16 ps) used by Peon et al.[31] to fit their data for monellin.

Contribution from Bulk and Surface-Bound Water. Previous experiments on the ultrafast spectral shift dynamics of monellin have included a 16 ps term to fit the spectral shift correlation function.[31,47] This observation, with the aid of MD simulations, led to the hypothesis that surface-bound ("biological") water does not contribute to the relaxation; the slow component represents the average rate of exchange of bound with unhindered bulk water, which contributes the ∼1 ps relaxation time. The simulations leading to Figure 7 provide an opportunity to examine what a typical MD force field says directly concerning this model. We have analyzed the contribution from individual residues and water molecules to the relaxation as a function of time and distance, using the method described previously.[39] The results indicate that virtually the entire shift (at only 1 ps after excitation) is contributed by waters that could be considered "surface-bound" by the criterion of distance from the surface of the protein. The largest contributions come from waters that are in contact with the π electrons of the indole ring and are part of a network of H-bonded waters anchored by waters that are bound to a few strong H-bond partners. As expected, the anchor waters do not exchange significantly during a 1 ps time interval, nor do they make significant contributions to the shift. However, the waters in contact with the face of the indole ring exhibit rotational dynamics that are much closer to those of bulk water. Figure 8 captures this behavior by showing a plot of the accumulated average shift contribution by waters 1 ps after excitation as a function of center−center distance between Trp 3 and water.

Lifetime Heterogeneity in Monellin. Lifetime heterogeneity on a short time scale is not unreasonable for Trp3 of monellin. The environment near Trp3 is unusually rich in possibilities for lifetime heterogeneity, with at least *four* plausible candidates for electron acceptors in an electron transfer (ET) fluorescence quenching process. In addition to the usual nearby backbone amides, two other amides are transiently quite close to Trp3: the backbone amide of Gly1 and the side chain amide of Gln59. The latter two are particularly potent because of the positioning of nearby positive charges that are close to the acceptor yet fairly distant from the Trp ring. Furthermore, these quenchers on relatively disordered groups provide large fluctuations in ET rate.

We have carried out QM−MD trajectories to predict the ET quenching propensity for the four amides by the recently published method.[44−46] Figure 9 displays the CT and ^1L_a transition energies computed by INDO/S-CI during 50 ps trajectories for the case in which the QM fragment contains the backbone amides of Gly1, Glu2, and Trp3. The energy gap varies considerably during the trajectory. About 65% of the time, the lowest CT state is on Gly1. The remainder of the time it resides mainly on the Trp and occasionally on Glu2. Most pertinent, however, is that 100% of the large downward fluctuations in the CT energy in Figure 9 that cross ^1L_a are for electron transfer to the amide on Gly1. Comparison with a trajectory in which the energy of charge transfer to the side chain amide of Gln59 is surveyed (not shown) shows similarly low-energy CT states for transfer to the side chain amide of Gln59, although the occurrence is much less than for transfer to Gly1.

Compared to monellin, IIA^{Glc} exhibits a remarkably long lifetime, nearly the longest expected, based on that of 3-meth-

(47) Pal, S. K.; Peon, J.; Zewail, A. H. *Proc. Natl. Acad. Sci. U.S.A.* **2002**, *99*, 1763.
(48) Toptygin, D.; Brand, L. *Chem. Phys. Lett.* **2000**, *322*, 496.

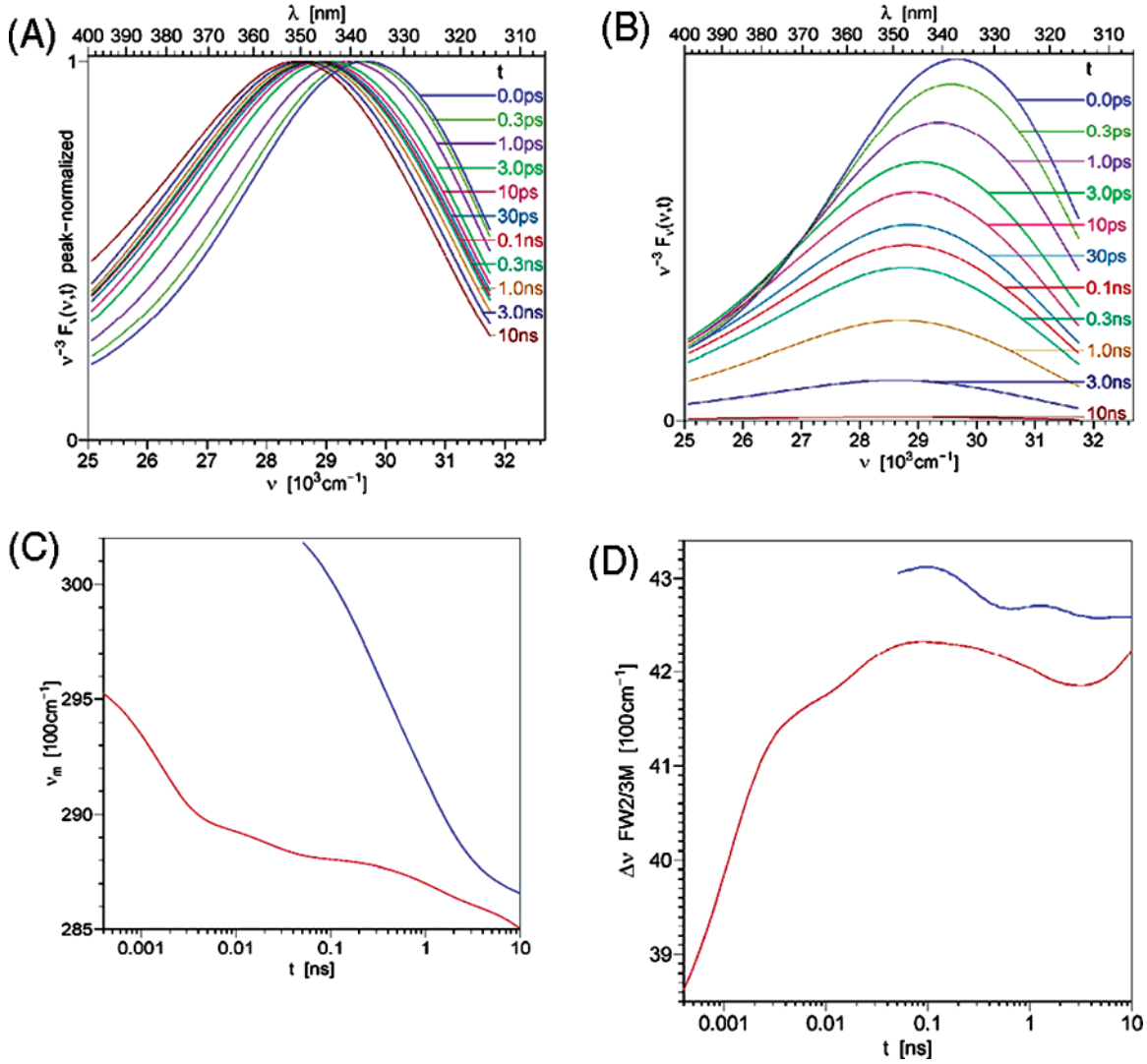

Figure 6. Monellin's normalized TRES (A), non-normalized TRES (B) across the full scale from 0.3 ps to 10 ns, and the spectral maximum versus time (C), spectral width versus time (D). Blue lines in panels C and D show TCSPC indole/glycerol results. That solvent relaxation proceeds smoothly with little change in energy width (see text).

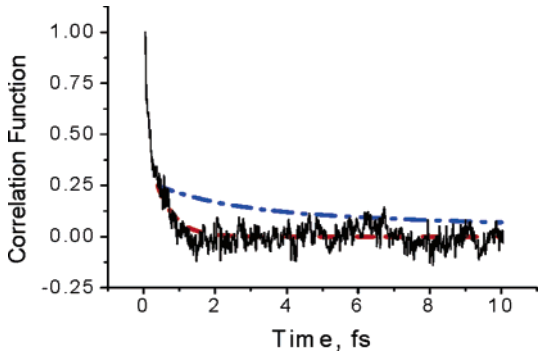

Figure 7. Simulation of correlation function, $C(t)$, for spectral shift following excitation from the average of 26 QM−MM trajectories of solvated monellin at 300 K (black solid). Single exponential with $\tau = 500$ fs starting at 400 fs (red dashed). The $C(t)$ of ref 31, equal amplitudes with $\tau = 2$ and 16 ps starting at 400 fs (blue dash-dot).

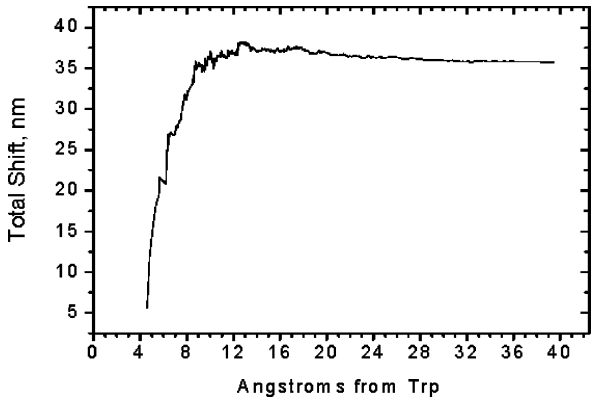

Figure 8. Plot of total fluorescence red shift 1 ps after excitation averaged over trajectories of Figure 7 contributed by all water lying closer than the distance indicated on the abscissa.

ylindole. A simulation similar to that for monellin is shown for IIA^{Glc} in Figure 10. Comparing Figures 9 and 10, one sees that the average CT−^1L_a gap is considerably larger for Trp 21 of IIA^{Glc} compared to Trp 3 of monellin. This is reasonable considering the unusual electrostatic environment found for Trp21 which is in what could be considered a cation−π complex with Arg 165 on one side of the indole ring. There are no nearby charged groups in the direction of electron transfer from the Trp ring toward the Trp backbone amide. Another large difference between the two is the amplitude of fluctuation in

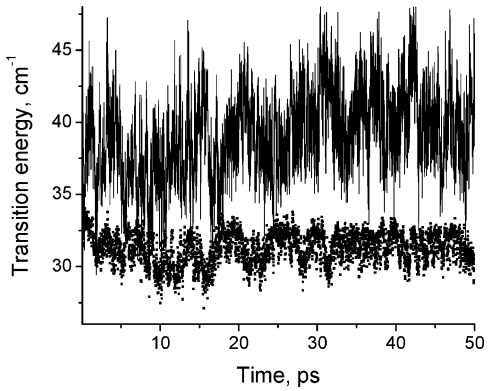

Figure 9. Simulation of lowest CT (line) and ^1L_a (points) state transition energies for monellin during a single 50 ps QM−MD simulation in which the possible CT states include the Gly1 amide as well as the local Trp amides as acceptor. Note the large fluctuations with several picosecond relaxation times.

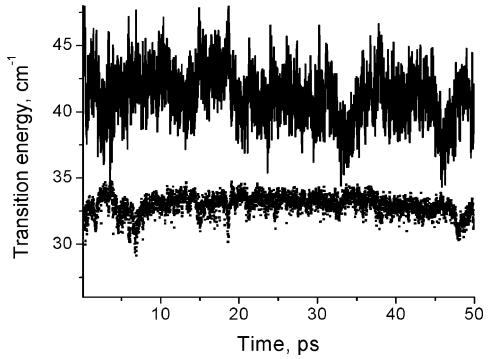

Figure 10. Simulation of lowest CT (line) and ^1L_a (points) state transition energies for IIA^{Glc} during a single 50 ps QM−MD simulation. The possible CT states include only the local Trp amides as acceptors because no other candidates are likely.

the CT energy. During the trajectory, the CT energy for monellin varies by about 20 000 cm^{-1} (2.5 eV) in contrast to that for IIA^{Glc}, where the variation is only 14 000 cm^{-1}, with the extremes being considerably more transient than for monellin. The large fluctuations for monellin arise because Trp3 resides so close to the N-terminus. The terminal positively charged ammonium group greatly stabilizes electron transfer to the Gly1 amide group (typically 1.5−2 eV). Significantly, during the monellin trajectory, the CT energy is much lower during the first 25 ps than during the last 25 ps, with the transition occurring over about 10 ps. This suggests that a significant subpopulation of the excited ensemble may undergo electron transfer quenching at much higher rate than the average. This provides an alternative source of decay microheterogeneity to the strict "rotamer" mechanism.

Conclusions

The ultrafast photophysics of Trp in the proteins monellin and IIA^{Glc} has been studied using time-resolved fluorescence spectroscopy with both picosecond and femtosecond time resolution. Trp in monellin exhibits a multiexponential fluorescence decay beyond the water relaxation of ∼1.2 ps. This multiexponentiality is likely associated with ground-state heterogeneity due to different conformers, including a rapidly quenched ensemble of Trp. The corresponding decay associated spectra of these states have been extracted from the data. In addition to ∼0.6, 2.2, and 4.2 ns lifetimes, a very fast lifetime of ∼16 ps was found in monellin. The decay associated spectrum of this fast component has a positive amplitude at all detected wavelengths and is comparable in shape and position to other components, leading to TRES widths that increase nonuniformly after 5 ps. This indicates that this 16 ps component originates from ground-state heterogeneity, and not from solvent relaxation alone. This is supported by analysis of the MD (QM−MM) simulations, which indicate that a large fraction of the shift comes from surface-bound water and is virtually complete within 1 ps. Much of this fast relaxation can be attributed to nearby charged residues. We note that the spectral relaxation features described above can also be seen in previously published TRES.[31] We have continued simulations and begun transient absorption studies to better understand the physical origins (i.e., electron transfer) of the highly quenched 16 ps conformer. Upconversion clearly opens new windows into the Trp microenvironment of proteins, and clarified photophysical mechanisms should help bring us improved data about rapid, short-range structural fluctuations.

Acknowledgment. This research was supported, in part, by the Intramural Research Program of the NIH, NHLBI. This work was also supported by NIH Grant GM-38759 and by NSF Grants MCB-0133064, MCB-0416965, and MCB-0446542. The authors thank Dr. Tiqing Liu for some of the monellin ET trajectories. We also thank Mary D. Barkley and J. B. Alexander Ross for helpful discussions about Trp photophysics.

Note added in proof. At the time this paper was submitted, we learned of simulation work in press by Nillson and Halle (*PNAS* **2005**, *102*, 13867) that also questions the interpretation of monellin's 16 ps exponential term via water dissociation. They also describe protein dynamics on a slightly longer time scale with lower $C(t)$ amplitude than Peon et al., and our current work does not contradict their new findings. We only assert the importance of measured heterogeneity in the emission surface.

JA055746H